Journal of Cellular Biochemistry 75:118–129 (1999)

Myosin Translocation in Retinal Pericytes During Free-Radical Induced Apoptosis

Negin Shojaee,[1] **Wayne F. Patton,**[2] **Herbert B. Hechtman,**[3] **and David Shepro**[1]*

[1]Microvascular Research Laboratory, Biological Science Center, Boston University, Boston, Massachusetts 02215
[2]Bioanalytical Assay Development, Molecular Probes, Inc., Eugene, Oregon 97402
[3]Department of Surgery, Harvard Medical School, Boston, Massachusetts 02214

Abstract Vascular pathologies induced by ischemia/reperfusion involve the production of reactive oxygen species (ROS) that in part cause tissue injury. The production of ROS that occurs upon reperfusion activates specific second messenger pathways. In diabetic retinopathy there is a characteristic loss of the microvascular pericyte. Pericytes are more sensitive than endothelial cells to low concentrations of ROS, such as hydrogen peroxide (H_2O_2) when tested in vitro. Whether the pericyte loss is due to toxic cell death triggered by the noxious H_2O_2 or apoptosis, due to activation of specific second messenger pathways, is unknown. During apoptosis, a cell's nucleus and cytoplasm condense, the cell becomes fragmented, and ultimately forms apoptotic bodies. It is generally assumed that apoptosis depends on nuclear signaling, but cytoplasmic morphological processes are not well described. We find that exposing cultured retinal pericytes to 100 µM H_2O_2 for 30 min leads to myosin heavy chain translocation from the cytosol to the cytoskeleton and a significant decrease in cell surface area. Pericyte death follows within 60–120 min. Exposing cells to 150 mJ/cm^2 ultraviolet radiation, an alternate free radical generating system, also causes pericyte myosin translocation and apoptosis. Proteolytic cleavage of actin is not observed in pericyte apoptosis. 3-aminobenzamide, a pharmacological inhibitor of the cleavage and activation of the DNA-repairing enzyme poly (ADP-ribose) polymerase (PARP) inhibits pericyte apoptosis, and prevents myosin translocation. Deferoxamine, an iron chelator known to interfere with free radical generation, also inhibits pericyte myosin translocation, contractility, and cell death. Myosin translocation to the cytoskeleton may be an early step in assembly of a competent contractile apparatus, which is involved in apoptotic cell condensation. These results suggest that pericyte loss associated with increased free radical production in diabetic retina may be by an apoptotic phenomenon. J. Cell. Biochem. 75:118–129, 1999.

Key words: myosin translocation; apoptosis; ischemia actin

Apart from acting as noxious toxins that indiscriminately affect biological processes, reactive oxygen species (ROS) appear to play significant physiological roles in inflammatory induced intracellular signal transduction pathways, both as primary and secondary messengers [Suzuki et al., 1997; Lander, 1997; Hastie et al., 1997a,b]. ROS act as primary messengers when they directly activate or inhibit intracellular second messenger cascades, such as the phospholipase C, phospholipase D, or adenylate cyclase pathways [Natarajan et al., 1993; Hastie et al., 1997a,b]. In endothelial cells, micromolar concentrations of H_2O_2 inhibit the adenylate cyclase and activate the phospholipase D pathways that lead to translocation of junction-associated nonmuscle filamin, rearrangement of cytoskeletal F-actin, and increases in intercellular permeability [Hastie et al., 1997a,b]. ROS function as second messengers when a ligand-receptor interaction produces ROS, which subsequently affect specific signal transduction pathways. Upon stimulation of vascular smooth muscle cells with platelet-derived growth factor (PDGF), intracellular H_2O_2 levels rise, tyrosine phosphorylation increases, mitogen-activated protein kinase is stimulated, and DNA synthesis increases [Sundaresan et al., 1995]. All of these PDGF-mediated responses are blocked by free radical scavengers. Other agonists, such as epidermal growth factor, interleukin-1, tumor

Grant sponsor: National Institutes of Health; Grant numbers: HL-98553, 56618, GM-2489, and 35141.

*Correspondence to: Dr. David Shepro, Microvascular Research Laboratory, Boston University, 5 Cummington Street, Boston, MA 02215. E-mail: shepro@bu.edu

Received 21 October 1998; Accepted 6 April 1999

necrosis factor, transforming growth factor-b1, and angiotensin II are known to produce H_2O_2 as an integral step in their respective receptor signaling pathways [Bae et al., 1997; Suzuki et al., 1997; Lander, 1997].

Oxidant stress induced free radical formation is known to trigger apoptosis [Lander, 1997; Sarafian and Bredsen, 1994; Slater et al., 1995]. Apoptosis is a physiological type of cell death. Blood cells, for instance, undergo continuous renewal from hematopoietic progenitor cells. In contrast neurons have a limited capacity for self-renewal and most survive for the life of the organism. Though several kinases, phosphatases, proteases, and phospholipases are implicated in ROS-mediated signaling pathways, ultimate downstream protein targets are poorly defined. The nucleus is not the sole target of apoptosis, and programmed cell death can proceed in enucleated cells [Jacobson et al, 1994; Lu et al., 1996]. While a morphological change in the cytoplasm is recognized as an early hallmark of apoptosis, the morphological process is only vaguely described as "cell shrinkage, cell volume loss, cytoplasmic condensation, or contraction," without rigorous delineation of the necessary modifications in the cytoplasm required to invoke the event [Wood and Youle, 1994; Kroemer et al., 1995; Chuang et al., 1997]. The ultrastructural alterations in the cytoplasm arising from apoptosis are often considered nonspecific and are poorly characterized [Kroemer et al., 1995]. Consequently, the cytoskeletal proteins responsible for the event are not yet defined and are the focus of the research in this report.

A pathological characteristic of diabetic retinopathy is the loss of pericytes from the microvasculature. Increased free radicals generated under hyperglycemic conditions could damage the retina. A significant restoration of pericytes by trolox, an amphipathic antioxidant, suggests the involvement of oxidative injury during pericyte loss in diabetic retinopathy [Asnsari et al., 1998; Hallberg et al., 1996]. ROS are known to induce apoptosis in vascular smooth muscle cells as well as pericytic mesangial kidney cells [Li et al., 1997; Sugiyama et al., 1996; Sandau et al., 1997; Baker et al., 1994].

This report demonstrates that cultured bovine retinal pericytes undergo apoptosis after exposure to either H_2O_2 or ultraviolet radiation. Moreover free radical-induced pericyte apoptosis is associated with subcellular redistribution of myosin. Myosin translocates from the cytosol to the cytoskeleton within 30 min of exposure to 100 μM hydrogen peroxide or 150 mJ/cm^2 ultraviolet radiation (UV-C). The translocation is inhibited by the free radical scavenger deferoxamine or the poly (ADP-ribose) polymerase inhibitor 3-aminobenzamide. ROS-induced cytoplasmic condensation appears to be a myosin-based event in retinal pericytes that precedes programmed cell death.

MATERIALS AND METHODS

Cell Isolation and Culture

Retinal pericytes are derived from isolated bovine retinal microvessels as described by Gitlin and D'Amore [1983]. Briefly, pericytes are isolated from calf retinas by thoroughly mincing them and digesting with 0.1% Collagenase 2 (Worthington Enzymes, Freehold, NJ)/0.1% BSA (ICN Pharmaceuticals, Irvine, CA) in PBS, Ca^{2+} and Mg^{2+} free (2 ml per retina) for 30 min at either room temperature or 37°C. Tissue is passed through a 100 um nylon mesh (Tetko, Briarcliff Manor, NY) and resuspended in media containing 10% fetal calf serum (Hyclone, Logan, UT), 2 mM L-glutamine (Gibco, Grand Island, NY), 1% Antibiotic-Antimycotic (Sigma Chemicals, St. Louis, MO) in Dulbecco's modified Eagle medium (D-MEM, Gibco). Cells are seeded onto tissue culture plates at 11 cm^2 per retina and kept in a humidified incubator at 37°C/5% CO_2. Media are replaced twice per week. Pericytes are identified by their nonepithelial cell, stellate morphology, lack of contact inhibition, positive staining for smooth muscle actin, lack of staining for factor VIII, and lack of staining with fluorescently labeled acetylated low-density lipoprotein.

HL-60 cells are maintained in continuous suspension culture as previously described [Mitchell et al., 1986]. Cells are grown to late log phase, 1×10^6 cells/ml, and then diluted to 2×10^5 cells/ml for further propagation. Cells are treated with 1.3% DMSO or 10^{-6} M retinoic acid followed by 6×10^{-5} M dimethylformamide a day later. Cells are exposed to the reagents for 1–5 days to obtain maximally differentiated granulocytic cells. Monocyte/macrophage differentiation is induced by addition of 1×10^{-8} M 12-O-tetradecanoylphorbol-13-acetate (TPA, Sigma, 1 mg/ml in DMSO).

Pericyte Treatment With Inducers and Inhibitors of Apoptosis

Prior to the experiments pericytes are kept in a serum free media containing 1% BSA (Sigma Chemicals), 2 mM L-glutamine (Gibco), 1% Antibiotic-Antimycotic (Sigma Chemicals), 1% ITS (Sigma Chemicals) in DMEM for 24 h.

Pericytes are treated with H_2O_2 for times ranging from 5 min to 1 h, and doses ranging from 50 µM to 500 µM. In some experiments cells are pretreated with 5 mM 3-aminobenzamide (an inhibitor of poly[ADP-ribosyl] polymerase) for 45 min. Ultraviolet irradiation is performed with a UV crosslinker (Spectrolinker, Westbury, NY). Cells are irradiated with 150 mJ/cm^2 of UV-C light and different subcellular fractions are collected after a 1 h or 3 h recovery period.

Apoptosis Assays

Pericytes are grown in 96-well plates and treated with H_2O_2. Decreased mitochondrial activity is measured by methylthiazol tetrazolium (MTT) assay as described by Hastie et al. [1997a].

An early indicator of apoptosis is the redistribution of phosphatidylserine on the outer leaflet of the plasma membrane, a process that can be detected by the binding of Annexin V, a member of a family of proteins that binds to acidic phospholipids. For detection of exposed phosphatidylserine in subpopulation of cells, pericytes are incubated with FITC-labeled annexinV (Clontech, CA) and analysed using an inverted IM-35 Zeiss fluorescent microscope. After exposure to 100 µM H_2O_2, pericytes are collected by trypsinization and resuspended in binding buffer, and stained with FITC-labeled annexin V (1 mg/ml) and propidium iodide (2.5 mg/ml) for 10 min.

Preparation of Cell Lysates and Subcellular Fractions

Pericytes are fractionated into cytosol, membrane/organelle, nucleus, and cytoskeleton fractions as previously described [Ramsby et al., 1994; Shojaee et al., 1998]. Pericytes seeded onto 100-mm culture dishes are rinsed twice with PBS (Ca^{2+}/Mg^{2+} free) and extracted in ice-cold digitonin buffer (0.01% digitonin, 10 mM PIPES, pH 6.8, 300 mM sucrose, 100 mM NaCl, 3 mM $MgCl_2$, 5 mM EDTA, and protease inhibitors (5 mM ethylene glycol-bis [β-aminoethyl ether] N,N,N'N'-tetra acetic acid [EGTA], 1 ug/ml leupeptin, 1 mM phenylmethylsulfonyl fluoride [PMSF], and 0.11 IU aprotinin). The cells are incubated on ice with gentle agitation for 10 min. The supernatant (cytosolic fraction) is collected and the residual cell components are sequentially extracted in Triton X-100, Tween-40/deoxycholate, and then SDS. Triton X-100 extraction is performed for 30 min in 0.5% Triton X-100, 10 mM PIPES, pH 7.4, 300 mM sucrose, 100 mM NaCl, 3 mM $MgCl_2$, 3 mM EDTA, protease inhibitors. After the supernatant (membrane/organelle fraction) is collected, the residual material is extracted on ice for 10 min with a Tween-40/deoxycholate buffer, containing 1% Tween 40, 0.5% deoxycholate, 10 mM PIPES, 1 mM MgCl2, 10 mM NaCl, pH 7.4, and protease inhibitors. The supernatant (nuclear fraction) is collected, and 100°C SDS buffer, containing 2.5% SDS in 10 mM Tris-HCl, pH 8 and protease inhibitors, is added to solubilize the cytoskeleton fraction. The culture dish is scraped and chilled on ice. Fifty ul of chilled sample buffer II containing 10 mM Tris-HCl, pH 8.0; with 1 mg/ml DNase I and 0.25 mg/ml RNase A; 50 mM $MgCl_2$ is added to the culture dish and the dish is incubated on ice for 5 min. The cytoskeletal fraction is collected and heated at 100°C for 5 min. All subcellular fractions are then acetone-precipitated in ice-cold acetone (final concentration 80%) and redissolved in equal volumes of sample buffer containing 0.1 M Tris-acetate (pH7.0), 2% SDS, 5% mercaptoethanol, 5% sucrose, 0.025% Bromophenol blue.

Electrophoresis, Immunoblotting, and Protein Quantification

Subcellular fractions, solubilized in a sample buffer of 0.1 M Tris-acetate (pH 7.0), 2% SDS, 5% Mercaptoethanol, 5% sucrose, and 0.025% Bromophenol blue are subjected to 5% SDS-polyacrylamide gel electrophoresis according to manufacturer's protocol (Genomic Solutions, Chelmsford, MA). Equal volume of protein is loaded in each lane to determine the subcellular distribution of myosin. After electrophoresis, proteins are electroblotted to 0.4 um pore size nitrocellulose membrane for 1 h (BioRad, Hercules, CA). After electroblotting the membrane is incubated in blocking buffer containing 5% BSA, 0.1% Tween-20 for at least 1 h, followed by incubation in 1:500 dilution of mouse anti-human smooth-muscle myosin antibody

(Sigma). The membrane is then incubated in alkaline phosphatase-conjugated goat anti-mouse IgG (Cappel, Durham, NC) and myosin bands are visualized using a nitroblue tetrazolium/5-bromo-4-chloro-3-indoylphosphate p-toluidine chromogen system (Sigma) (Shojaee et al., 1998).

High resolution two-dimensional gel electrophoresis is performed as previously described [Patton et al., 1990] using the ESA Investigator 2-D Electrophoresis System (Genomic Solutions). To improve reproducibility of the focusing gel and prevent its stretching or breaking during transfer to the second dimension, a 0.08 mm thread is incorporated along the length of the tube prior to polymerization of the gel matrix [Patton et al., 1990]. The second dimension electrophoretic separation is performed using a high tensile strength acrylamide-based matrix (Duracryl; Genomic Solutions) [Patton et al., 1992]. Proteins are visualized by silver staining as previously described [Rabilloud, 1992]. Images of electrophoresis gels are then obtained by digitizing gels at 1,024 × 1,024 pixels (picture elements) resolution with 256 grey scale levels using the charged coupled device (CCD) camera of the Bio Image 110S computerized imaging system from Genomic Solutions (Ann Arbor, MI). For nitrocellulose membranes, image acquisition is performed using a flat-bed scanner interfaced to an Apple Macintosh Power PC microcomputer. Quantitation of all images is performed with Bio Image software (BioImage, Ann Arbor, MI).

Immunofluorescence Microscopy

Pericytes seeded onto glass coverslips are rinsed three times with PBS (Ca^{2+}/Mg^{2+} free) and fixed in 1G4F, containing 99 ml formalin stock solution (0.9% NaCl in 10% buffered formalin solution) and 1 ml 25% aqueous glutaraldehyde for for 10 min at room temperature. Subsequently the cells are rinsed three times with PBS (Ca^{2+}/Mg^{2+} free) and permeabilized in 0.2% Triton X-100 in PBS for 10 min at room temperature followed by incubation in PBS containing 1 uM rhodamine phalloidin for 1 h. The excitation and emission wavelengths of rhodamine are 557 and 580 nm, respectively. The coverslips are mounted on slides in glycerol: H_2O (9:1) and sealed with nail varnish. The slides are monitored under an inverted IM-35 Zeiss fluorescent microscope. Five different fields of treated and untreated cells were evaluated by computerized morphometry. Cell area measurement is performed with NIH Image version 1.57 public domain software developed by Dr. W. Rasband, Research Services Branch, NIMH. The ratio corresponds to the cell area of control group divided by the treated group.

RESULTS

Reactive Oxygen Species-Induced Apoptosis in Retinal Pericytes

Retinal pericyte susceptibility to injury by reactive oxygen species (ROS) is evaluated utilizing a reoxygenation injury model previously described by our laboratory for endothelial cells [Hastie et al., 1997a,b]. Injury resulting from the exogenous addition of H_2O_2 is determined by measuring cleavage of the vital dye MTT (Fig. 1A). Loss of pericyte viability is readily apparent after 30 min exposure to 100 μM

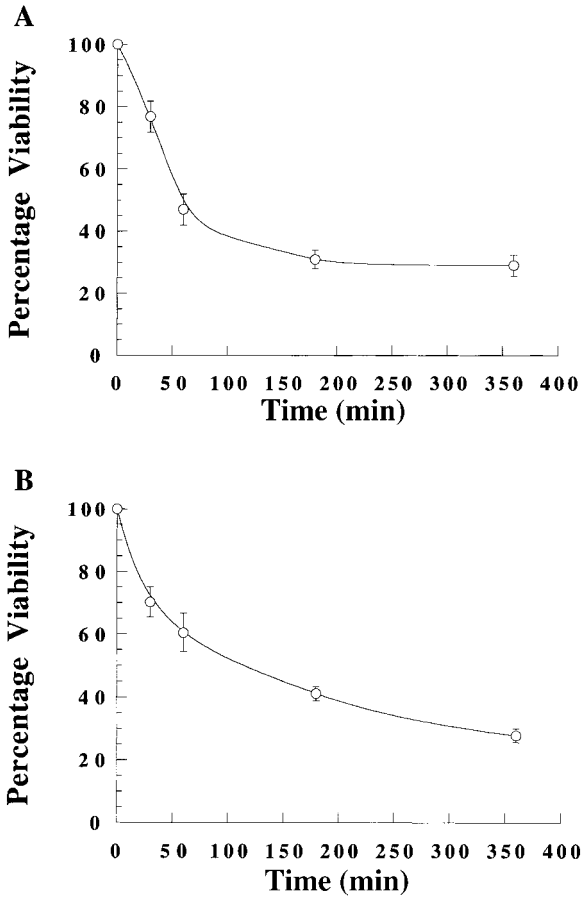

Fig. 1. ROS-induced cytotoxicity as measured by the MTT assay. Cells are exposed to 100 μM H_2O_2 (**A**) and 150 mJ/cm^2 UV light (**B**) for the indicated times. A: H_2O_2-induced injury is compared with untreated cells. B: UV light injury is compared with untreated cells. Error bars are means ± standard deviation (n = 6)

H_2O_2 as indicated by a 55% decrease in mitochondrial activity. Mitochondrial activity in human umbilical vein endothelial cells decreases to comparable levels after more than 2 h exposure to 100 μM H_2O_2 [Hastie et al., 1997a], which suggests that pericytes are more sensitive to H_2O_2 exposure than endothelial cells. Exposing cells to ultraviolet radiation is a commonly employed model system for inducing apoptosis through the generation of oxygen free radicals. Loss of viability is also apparent after exposing pericytes to 150 mJ/cm^2 of UV-C light and allowing them to recover in culture for varying lengths of time (Fig. 1B).

To establish that loss of pericyte viability observed utilizing the MTT assay is due to apoptosis, the appearance of phosphatidylserine on the extracellular face of the plasma membrane is monitored utilizing fluorescein isothiocyanate-conjugated annexin V. Redistribution of phosphatidylserine is a general feature of apoptosis, regardless of the initiating stimulus [Martin et al., 1995]. Annexin V binding to retinal pericyte membranes is evident after 60 min exposure to 100 μM H_2O_2. Cells exposed to H_2O_2 for 60 min are substantially more reactive to annexin V than cells exposed to H_2O_2 for 5 min (Fig. 2C,D). Cells not exposed to H_2O_2 are unlabeled with annexin V (data not shown). Minimal counterstaining of cells with propidium iodide indicates that the plasma membrane initially remains intact after exposure to H_2O_2 (Fig. 2E,F). In necrotic cells and late-stage apoptotic cells, the plasma membrane binds annexin V and the nucleus stains with propidium iodide.

An early morphological event observed typically in apoptosis is a rapid decrease in cell surface area. Exposing pericytes to 100 μM H_2O_2 results in a 3.5-fold decrease in cell surface area within 60 min. The H_2O_2-induced reduction in pericyte surface area is demonstrated by immunofluorescence microscopy of rhodamine-phalloidin stained cells (Fig. 3).

Reactive Oxygen Species-Induced Pericyte Apoptosis Causes Myosin Translocation

Changes in the subcellular distribution of myosin are evaluated by differential detergent fractionation (DDF). The amount of myosin in different subcellular compartments is obtained by DDF. Marker enzyme profiles confirm that the DDF procedure is suitable for isolating subcellular compartments in cultured retinal pericytes [Shojaee et al., 1998]. Subcellular fractionation of pericytes by the DDF technique indicates that myosin is found in four compartments (74% in the cytosol, 16% in the membrane/organelle, 3% in the nucleus, and 7% in the cytoskeleton). Vimentin, actin, and α-actinin are also distributed between these four subcellular compartments [Shojaee et al., 1998]. In control pericyte cultures, myosin is predominantly in the cytosol fraction (Fig. 4B). After exposing pericytes to 100 μM H_2O_2, the amount of myosin in the cytoskeleton increases, the amount of myosin in the cytosol decreases, and the amount of myosin in membrane/organelle and nuclear fractions remains unchanged (Fig. 4B). Translocation of myosin from the cytosol to the cytoskeleton occurs after exposing cells to 100 μM H_2O_2 for 30 min and gradually increases with time. When cells are exposed to 100 μM H_2O_2 for 60 min, 45% of the myosin is recovered in the cytoskeleton fraction and 41% in the cytosol (Fig. 4B). We consistently observe that myosin translocation involves redistribution between the cytosol and cytoskeleton compartments, with myosin levels in membrane/organelle and nucleus compartments remaining unaltered. Thus, data are presented with respect to cytosolic and cytoskeletal fractions in the remainder of the article. Immunoblotting of proteins from the four subcellular fractions with anti-smooth muscle myosin demonstrates that upon H_2O_2 stimulation the smooth muscle isotype of myosin translocates from the cytosol to the cytoskeleton compartment (Fig. 4A).

Pretreatment of pericytes for 60 min with 0.5 mM deferoxamine (an iron chelator that blocks free radical generation) prior to exposure to 100 μM H_2O_2 prevents myosin translocation from the cytosol to the cytoskeleton through 60 min (Fig. 5A). Deferoxamine pretreatment partially inhibits decreases in mitochondrial activity induced by H_2O_2 (100 μM) through 60 min (Fig. 5B). Treatment of pericytes with 5 mM 3-aminobenzamide (an inhibitor of PARP) for 45 min significantly inhibits myosin translocation from the cytosol to the cytoskeleton (Fig. 6A). Partial inhibition of H_2O_2-induced decreases in mitochondrial activity are also apparent (Fig. 6B).

Myosin translocation is also measured at different times after exposing pericytes to 150 mJ/cm^2 of UV-C light. Translocation of myosin from the cytosol to the cytoskeleton is detected

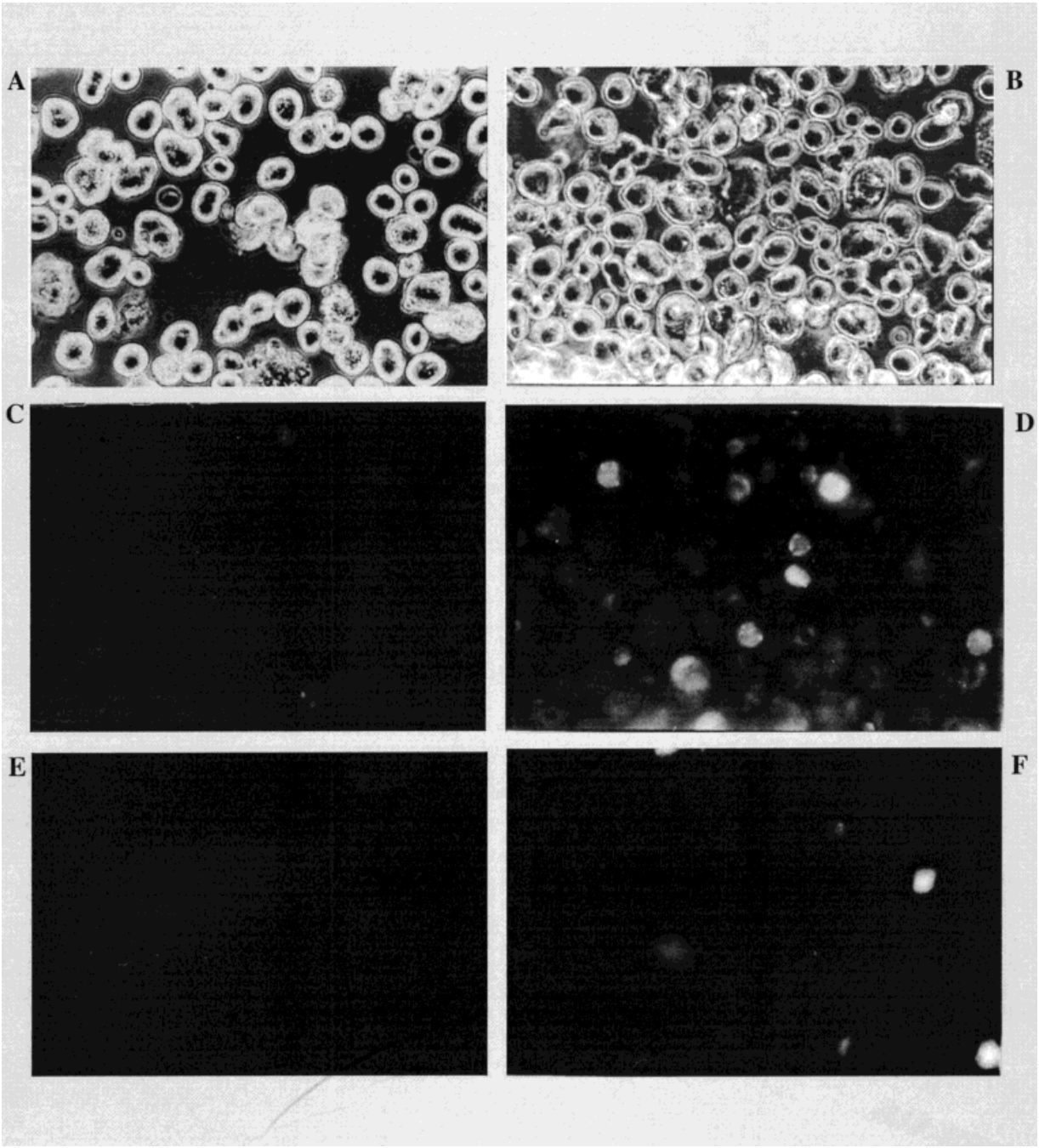

Fig. 2. Apoptosis is monitored by the binding of Annexin V to phosphatidylserine. Pericytes are exposed to 100 μM H_2O_2 for 5 and 60 min and subsequently visualized using FITC-labeled Annexin V. **A,B**: Phase contrast micrographs of pericytes treated with 100 μM H_2O_2 for 5 and 60 min, respectively. **C,D**: Annexin V labeled pericytes treated for 5 and 60 min, respectively, cells exposed to H_2O_2 are substantially more reactive to annexin V than cells exposed for 5 min. **E,F**: Propidium iodide labeled pericytes treated for 5 and 60 min, respectively; pericytes' plasma membranes remain intact and therefore they are not labeled with Propidium Iodide.

after 1 h post UV irradiation and gradually increases with time (Fig. 4C). Pretreatment of pericytes with 0.5 mM deferoxamine for 60 min prior to UV irradiation prevents myosin translocation from the cytosol to the cytoskeleton through 60 min (Fig. 7A). Treatment of pericytes with 5 mM 3-aminobenzamide for 45 min also significantly inhibits UV-induced myosin translocation from the cytosol to the cytoskeleton (Fig. 7B).

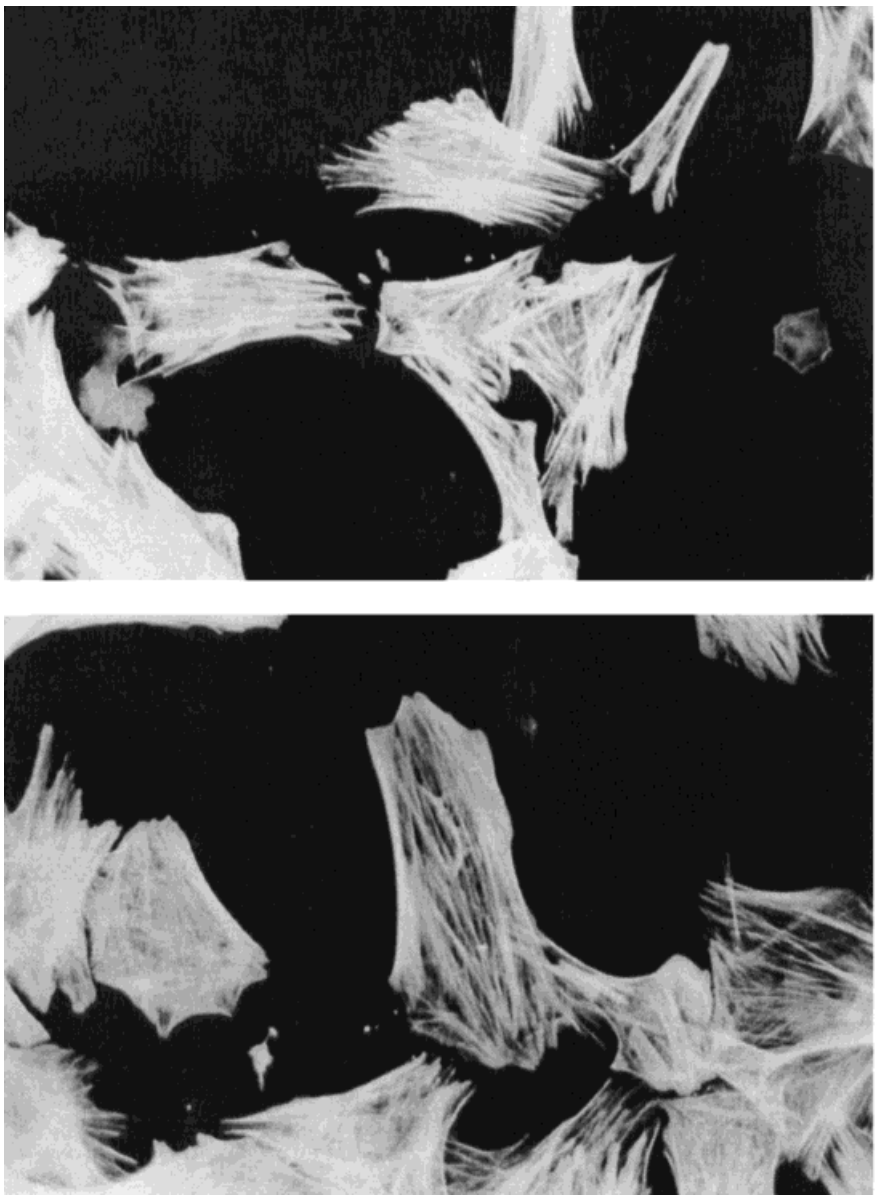

Fig. 3. H_2O_2-induced morphological changes are analyzed by immunofluorscence microscopy. F-actin is visualized using rhodamine-conjugated phalloidin. Pericytes surface area decreases upon their exposure to 100 μM H_2O_2 for 60 min (**A**) compared to untreated pericytes (**B**).

Reactive Oxygen Species-Induced Pericyte Apoptosis Does Not Lead to Proteolytic Cleavage of Actin

Several reports indicate that actin may be fragmented by specific proteases during apoptosis [Miyamoto and Wu, 1991; Mashima et al., 1995, 1997; Chen et al., 1996; Kayalar et al., 1996; Brown et al., 1997]. Actin fragmentation in response to H_2O_2 and UV irradiation is thus evaluated in retinal pericytes. HL-60 promyelocytic leukemia cells are utilized as a well characterized control cell type reputed to contain both native 42 kDa actin and the proteolyzed 38 kDa actin fragment. Compared to pericytes, HL-60 cells are relatively depleted in cytoskeletal proteins. Whereas actin represents 5% of the total protein in pericytes, HL-60 cells only contain 0.3% actin. Granulocytic differentiation of HL-60 cells, using 1.3% DMSO or 10^{-6} M retinoic acid followed by 6×10^{-5} M dimethylformamide at 24 h leads to a four fold increase in actin expression. Both the 42 kDa and 38 kDa actin species are readily observable by two-dimensional gel electrophoresis (Fig. 8D).

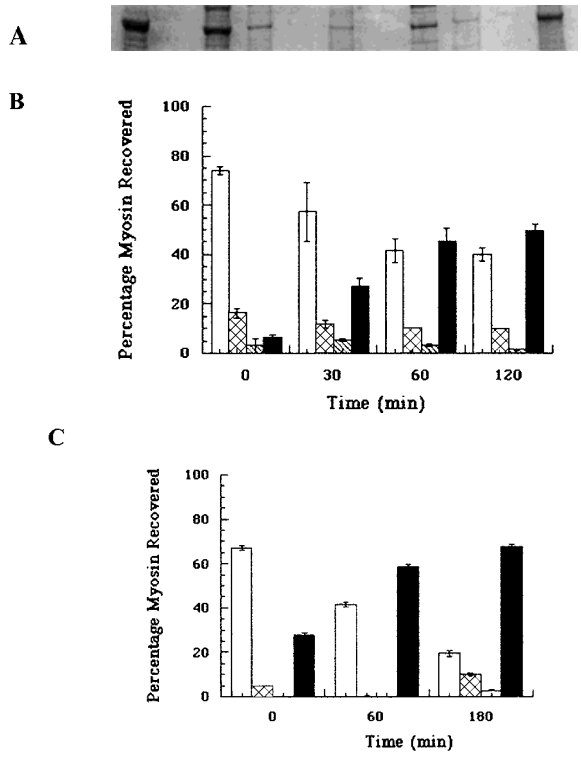

Fig. 4. Subcellular distribution of myosin in control, H_2O_2 (100 μM) and UV light (150 mJ/cm^2) treated cells. Cells are separated into cytosolic, membrane/organelle, nuclear, and cytoskeletal fractions. **B,C**: Bar graph depicting relative myosin concentration in each fraction after H_2O_2 (100 μM) and UV light (150 mJ/cm^2) exposure respectively. Cytosol fraction (hatched bars), membrane/organelle fraction (white bars), nuclear fraction (striped bars), cytoskeletal fraction (black bars). **A**: Electroblotted subcellular fractions are visualized with smooth muscle anti-myosin primary antibody as described in Materials and Methods. **Lanes 1** through **4** correspond to cytosolic, membrane/organelle, nuclear, and cytoskeletal fractions, respectively.

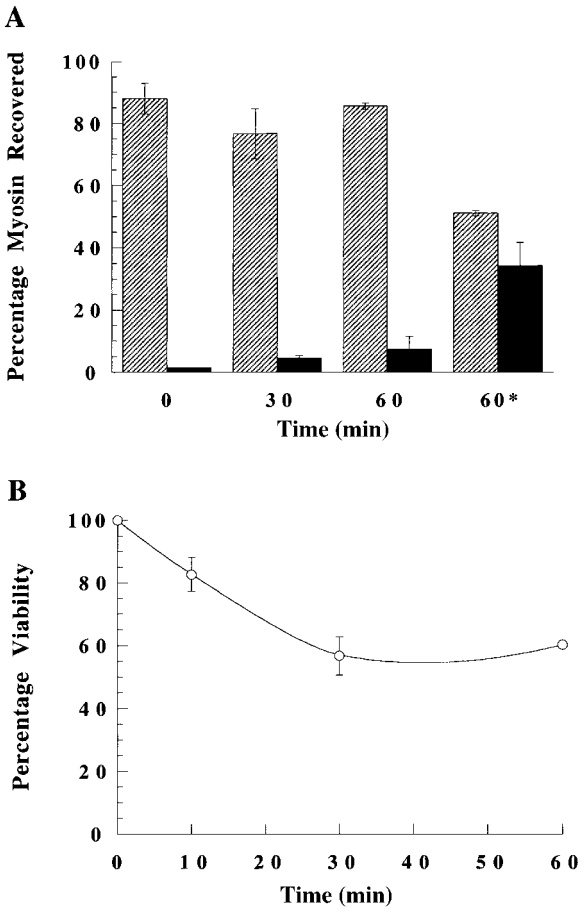

Fig. 5. Deferoxamine mediated protection from H_2O_2-induced myosin translocation and pericytes injury. **A**: Myosin distribution in cells pretreated with 0.5 μM deferoxamine for 60 min prior to 100 μM H_2O_2 for 30–60 min. **B**: Mitochondrial activity in cells pretreated with 0.5 mM deferoxamine for 60 min prior to exposure to 100 μM H_2O_2 for 10–60 min. Cytosol fraction (hatched bars), cytoskeletal fraction (black bars). *60 min exposure to 100 μM H_2O_2 in the absence of Deferoxamine.

The identity of the two proteins is confirmed by Edman-Based protein sequencing (data not shown). Exposing pericytes to 100 μM H_2O_2 for 1 h or 150 mJ/cm^2 of UV-C light followed by a 1 h incubation period in culture does not lead to the formation of a 38 kDa proteolytic actin fragment (Fig. 8A–C). One dimensional SDS-polyacrylamide gel electrophoresis, electroblotting to nitrocellulose membrane and probing the membrane with anti-actin antibody, confirms the presence of a single 42 kDa actin species in retinal pericytes exposed to H_2O_2 or UV radiation (data not shown). Thus, while translocation of myosin from the cytosol to the cytoskeleton occurs in ROS-induced pericyte apoptosis, proteolytic cleavage of actin is not observed.

DISCUSSION

Cytoskeletal proteins coordinate many interactions related to mural cells maintenance of the microvascular barrier including: signal transmission, cell motility, cell-cell apposition, and cell-substratum attachments [Gottlieb et al., 1991; Hitt and Luna, 1992; Shepro and Morel, 1993]. Microvessel endothelial cell and pericyte cytoskeletal proteins are also early and primary targets of second messenger cascades generated in response to inflammatory agonists such as ROS [Hastie et al., 1997a,b; Shepro and Morel, 1993]. This study begins to define a role of ROS in modifying the pericyte cytoskeleton as observed during apoptosis.

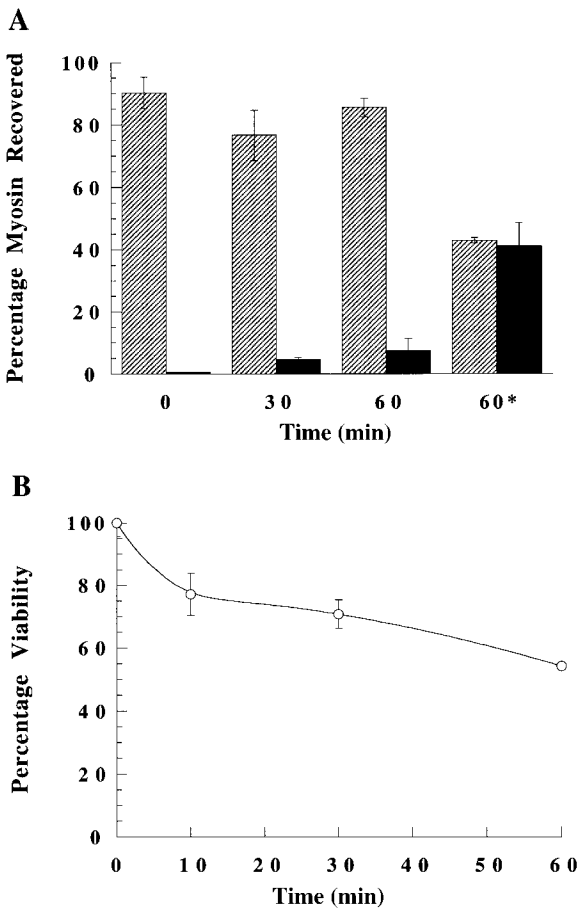

Fig. 6. 3-Aminobenzamide mediated protection from H_2O_2-induced myosin translocation and pericytes injury. **A**: Myosin distribution in cells pretreated with 5 mM 3-Aminobenzamide for 45 min prior to 100 μM H_2O_2 for 30–60 min. **B**: Mitochondrial activity in cells pretreated with 5 mM 3-Aminobenzamide for 45 min prior to exposure to 100 μM H_2O_2 for 10–60 min. Cytosol fraction (hatched bars), cytoskeletal fraction (black bars). *60 min exposure to 100 μM H_2O_2 in the absence of 3-Aminobenzamide.

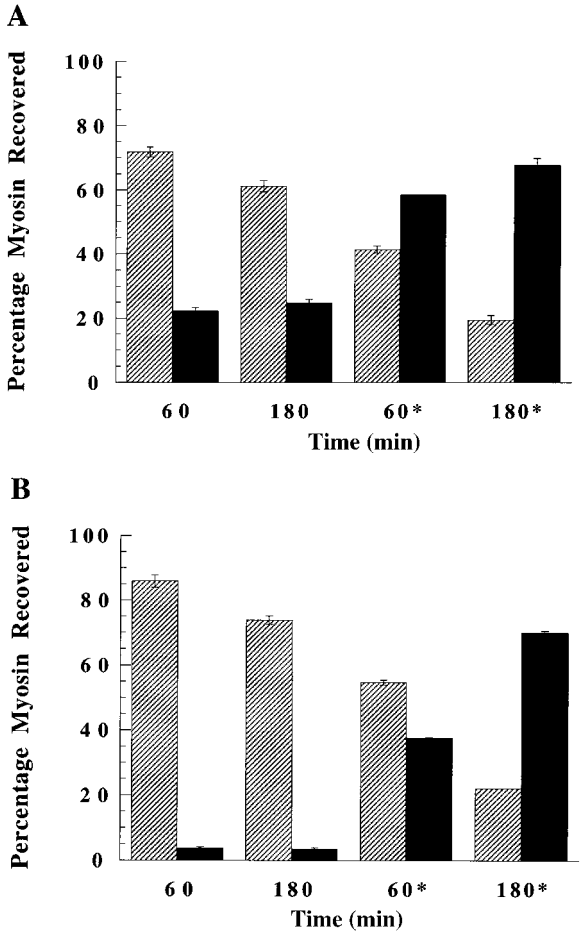

Fig. 7. **A**: Deferoxamine mediated protection from UV-induced myosin translocation. Myosin distribution in cells pretreated with 0.5 mM deferoxamine for 60 min prior to UV light exposure. **B**: 3-Aminobenzamide mediated protection from UV-induced myosin translocation. Myosin distribution in cells pretreated with 5 mM 3-Aminobenzamide for 45 min prior toUV light exposure. Cytosol fraction (hatched bars), cytoskeletal fraction (black bars). *60, *180 min exposure to UV light above.

Cytoplasmic changes accompanying apoptosis are well described but few studies address their molecular mechanisms. The characteristic decrease in cell volume is considered a secondary event to nuclear DNA fragmentation. However, many of the prototypical cytoplasmic changes that characterize apoptosis, induced by diverse stimuli such as granzymes A and B, Fas ligand, U.V. irradiation, staurosporine, and growth factor deprivation, do not require endonuclease-mediated nuclear DNA fragmentation or even a nucleus [Nakajima et al., 1995; Jacobson et al., 1994; Lu et al., 1996]. The literature is sparse about changes in myosin related to morphological changes with apoptosis. F-actin stress fiber interactions with myosin, which are in part regulated by the activation of myosin light chain kinase (MLCK), generate forces that mediate contraction/relaxation and other actin-based cytoskeletal responses in pericytes [Shepro and Morel, 1993]. In this study we focused on myosin redistribution in cell condensation related to apoptosis.

Activation of numerous cellular regulatory pathways is accompanied by the translocation of key proteins from one region of the cell to another. Cytoplasmic dynein undergoes intracellular redistribution concomitant with phosphorylation of the heavy chain in response to serum starvation and okadaic acid [Lin et al., 1993]. Soluble cytoplasmic myosin is translocated to the actin cytoskeleton during platelet

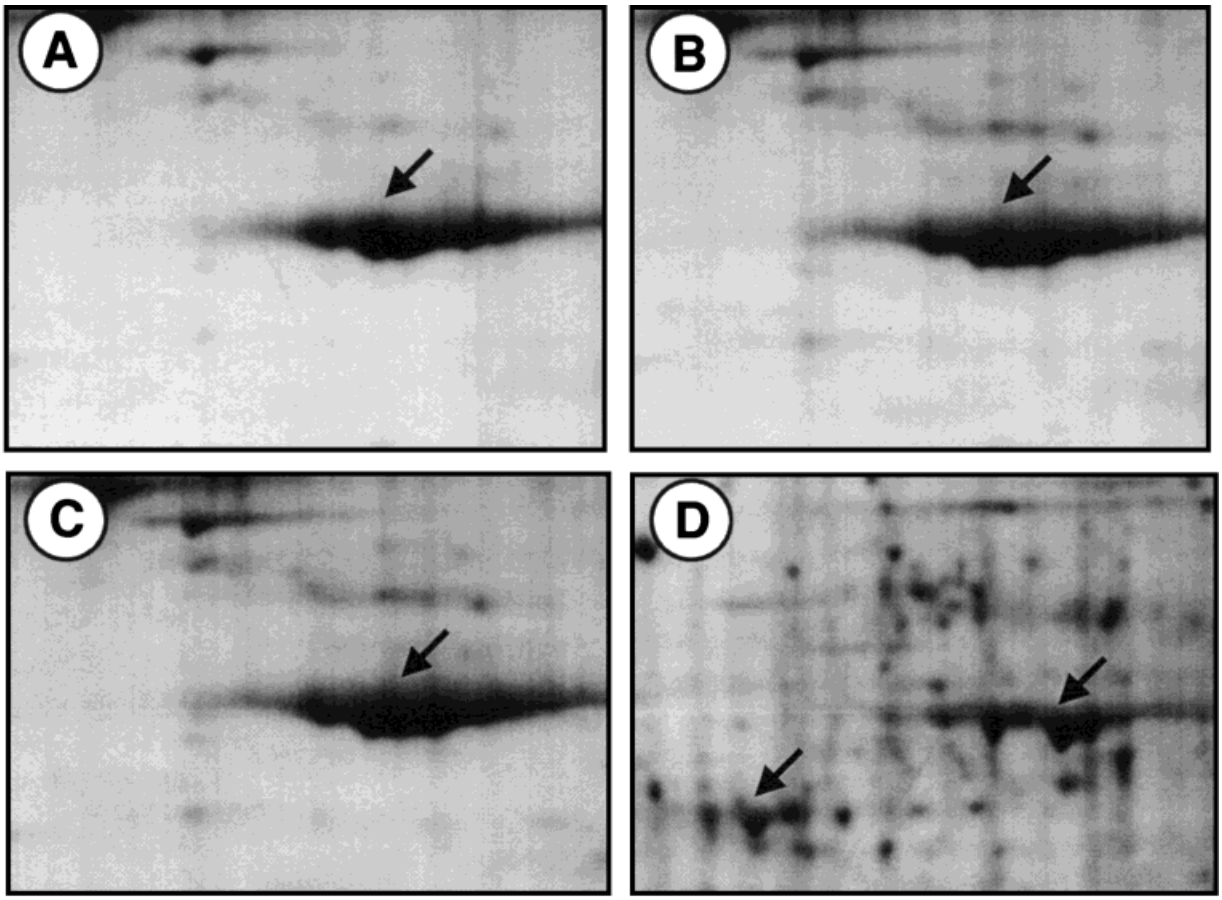

Fig. 8. Actin proteolysis in response to 100 μM H_2O_2 and UV irradiation in retinal pericytes is compared with HL-60 leukemia cells. **A**: Untreated pericytes, **B**: pericytes exposed to 100 μM H_2O_2 for 60 min, **C**: pericytes exposed to 150 mJ/cm^2 UV irradiation, **D**: HL-60 leukemia cells. In contrast to HL-60 cells (D) proteolytic cleavage of actin is not observed in H_2O_2 or UV light treated pericytes (B,C). Arrows indicate the position (s) of actin.

activation [Jennings et al., 1981]. Some investigators suggest that myosin light chain phosphorylation initiates myosin translocation and others have shown that myosin light chain phosphorylation can occur with the absence of myosin translocation. Additional evidence demonstrates that caldesmon enhances the binding of myosin to cytoskeletal actin upon platelet activation [Hemric et al., 1994]. The functional significance of this translocation is not established, although it occurs early during activation and correlates with shape change and aggregation.

In this study we demonstrate myosin redistribution in retinal pericytes during free-radical induced apoptosis. Myosin translocation coincides with cell contraction. Pretreatment of pericytes with deferoxamine and 3-aminobenzamide prior to free radical exposure inhibits myosin translocation and partially increases cell viability. Therefore, myosin heavy chain redistribution and association with the actin cytoskeleton in apoptotic retinal pericytes may orchestrate cell condensation at this early stage of apoptosis.

In contrast to myosin, actin has been intensively studied during apoptosis. The F-actin cytoskeleton is a likely cytoplasmic target of signaling cascades that leads to the morphological changes characteristic of apoptotic cells. Indeed, UV radiation- and etoposide-induced apoptosis in HL-60 promyelocytic leukemia cells is accompanied by early transient polymerization and later depolymerization of F-actin as well as changes in microfilament organization [Levee et al., 1996]. Some studies indicate that actin may be a target of intracellular proteolytic pathways activated during apoptosis. Activation of interleukin 1-beta converting enzyme (ICE) family proteases and subsequent cleav-

age of actin are reported during apoptosis [Mashima et al., 1995, 1997; Chen et al., 1996; Kayalar et al., 1996]. A 38 kDa, truncated actin isoform in HL-60 promyelocytic leukemia cells is thought to arise from specific proteolysis of the full length protein between valine-43 and methionine-44 [Miyamoto and Wu, 1991]. Actin is cleaved at the same site during spontaneous apoptosis of neutrophils in culture [Brown et al., 1997]. The observed cleavage site does not correspond to a consensus site for cysteine proteases of the ICE family but may arise from proteolysis by calpains since degradation is prevented by using a calpain inhibitor [Brown et al., 1997].

The actin molecule consists of two domains "small" and "large," which can be further subdivided into two subdomains [Kabsch et al., 1990]. Both the N-terminal and C-terminal reside in the small domain. The missing NH_2-terminus of p38 includes a large portion of subdomain 1 and part of subdomain 2 [Miyamoto and Wu, 1991]. This region of the molecule contains the known myosin-binding residues (Asp-24, Asp-26, Arg-28), as well as a portion of the binding region for DNase 1 (Arg-39, Gln-41, Val-43) and a site involved in actin fiber formation (His-40) [Suck et al., 1988; Holmes et al., 1990]. Thus, cleavage of actin at this site would be expected to inhibit rather than promote myosin association with the cytoskeleton. The universal role of actin degradation in the morphological changes associated with apoptosis is debatable since in vitro degradation of actin has not been observed in a number of intact cell types induced to undergo apoptosis utilizing a variety of stimuli [Song et al., 1997]. Our studies demonstrate that while readily observable in HL-60 cells, actin cleavage is not apparent during H_2O_2- or ultraviolet radiation-induced apoptosis of retinal pericytes (Fig. 8).

In summary, during ROS-induced pericyte apoptosis myosin translocates from the cytosol to the cytoskeleton with no proteolytic cleavage of actin. Translocation can be inhibited by deferroxamine, an oxygen free radical scavenger or 3-aminobenzamide, an inhibitor of the cleavage and activation of the DNA-repairing enzyme poly (ADP-ribose) polymerase.

ACKNOWLEDGMENT

We thank Dr. P. D'Amore (Harvard Medical School) for her scientific comments.

REFERENCES

Ansari NH, Zhang W, Fulep E, Mansour A. 1998. Prevention of pericytes loss by trolox in diabetic rat retina. J Toxicol Environ Health 54:467–475.

Bae Y, Kang S, Seo M, Baines I, Tekle E, Chock P, Rhee S. 1997. Epidermal growth factor (EGF)-induced generation of hydrogen peroxide; role in EGF receptor-mediated tyrosine phosphorylation. J Biol Chem 272:217–221.

Baker A, Mooney A, Hughes J, Lombardi D, Johnson R, Savill J. 1994. Mesangial cell apoptosis: the major mechanism for resolution of glomerular hypercellularity in experimental mesangial proliferative nephritis. J Clin Invest 94:2105–2116.

Brown S, Bailey K, Savill J. 1997. Actin is cleaved during constitutive apoptosis. Biochem J 323:233–237.

Chen Z, Naito M, Mashima T, Tsuruo T. 1996. Activation of actin-cleavable interleukin 1beta-converting enzyme (ICE) family protease CPP-32 during chemotherapeutic agent-induced apoptosis in ovarian carcinoma cells. Cancer Res 56:5224–5229.

Chuang T, Hahn K, Lee J, Danley D, Bokoch G. 1997. The small GTPase Cdc42 initiates an apoptotic signaling pathway in Jurkat T lymphocytes. Mol Biol Cell 8:1687–1698.

Freshney RI. 1994. Culture of animal cells. New York: Wiley-Liss.

Gottlieb A, Langille L, Wong M, Kim L. 1991. Biology of disease: structure and function of the endothelial cytoskeleton. Lab Invest 65:123–137.

Gitlin JD, D'Amore PA. 1983. Culture of retinal capillary cells using selective growth media. Microvasc Res 26: 74–80.

Hallberg CK, Trocme SD, Ansari NH. 1996. Acceleration of corneal wound healing in diabetic rats by the antioxidant trolox. Res Commun Mol Pathol Pharmacol 1:3–12.

Hastie L, W. Patton W, Hechtman H, Shepro D. 1997. Filamin redistribution in an endothelial cell reoxygenation injury model. Free Rad Biol Med 22:955–966.

Hastie L, Patton W, Hechtman H, Shepro D. 1997. H_2O_2-induced filamin redistribution in endothelial cells is modulated by the cyclic AMP dependent protein kinase pathway. J Cell Physiol 172:373–381.

Hemric ME, Tracy PB, Haerberle JR. 1994. Caldesmon enhances the binding of myosin to the cytoskeleton during platelet activation. J Biol Chem 269:4125–4128.

Hitt A, Luna E. 1994. Membrane interactions with the actin cytoskeleton. Curr Opin Cell Biol 6:120–130.

Holmes K, Popp D, Gebhard W, Kabsch W. 1990. Atomic model of the actin filament Nature 347:44–49.

Jacobson M, Burne J, Raff M. 1994. Programmed cell death and Bcl-2 protection in the absence of a nucleus. EMBO J 13:1899–1910.

Jennings LK, Fox JE, Edwards HH, Phillips DR. 1981. Changes in the cytoskeletal structure of human platelets following thrombin activation. J Biol Chem 256:6927–6932.

Kabsch W, Mannherz G, Suck D, Pai E, Holmes K. 1990. Atomic structure of the actin: DNase 1 complex. Nature 347:37–44.

Kayalar C, Ord T, Testa M, Zhong L, Bredesen D. 1996. Cleavage of actin by interleukin 1 beta-converting enzyme to reverse DNase I inhibition. Proc Natl Acad Sci USA 93:2234–2238.

Kroemer G, Petit P, Zamzami N, Vayssiere J, Mignotte B. 1995. The biochemistry of programmed cell death. FASEB J 9:1277–1287.

Lander H. 1997. An essential role for free radicals and derived species in signal transduction. FASEB J 11:118–124.

Levee M, Dabrowska M, Lelli J, Hinshaw D. 1996. Actin polymerization and depolymerization during apoptosis in HL-60 cells. Am J Physiol 271:C1981–C1992.

Li P, Dietz R, von Harsdorf R. 1997. Reactive oxygen species induce apoptosis of vascular smooth muscle cell. FEBS Lett 404:249–252.

Lin S, Collins C. 1993. Regulation of the intracellular distribution of cytoplasmic dynein by serum factors and calcium. J Cell Sci 105:579–588.

Lu M, Sato M, Cao B, Richie J. 1996. UV irradiation-induced apoptosis leads to activation of a 36-kDa myelin basic protein kinase in HL-60 cells. Proc Natl Acad Sci USA 93:8977–8982.

Martin S, Reutelingsperger C, Kuijten G, Keehen R, Pals S, van Oers M. 1995. Early redistribution of plasma membrane phosphatidylserine is a general feature of apoptosis regardless of the initiating stimulus: inhibition by overexpression of Bcl-2 and Abl. J Exp Med 182:1545–1556.

Mashima T, Naito M, Fujita N, Noguchi K, Tsuruo T. 1995. Identification of actin as a subsrtrate of ICE and an ICE-like protease and involvement of an ICE-like protease but not ICE in VP-16-induced U937 apoptosis. Biochem Biophys Res Commun 217:1185–1192.

Mashima T, Naito M, Noguchi K, Miller D, Nicholson D, Tsuruo T. 1997. Actin cleavage by CPP-32/apopain during the development of apoptosis. Oncogene 14:1007–1012.

Mitchell RL, Henning-Chubb C, Huberman E, Verma IA. 1986. c-fos expression is neither sufficient nor obligatory for differentiation of monomyelocytes to macrophages Cell 45:497–504.

Miyamoto S, Wu J. 1991. Identification of a 38-kDa protein (p38) in HL-60 leukemic cells as a truncated actin. Biochem Int 25:307–319.

Nakajima H, Golstein P, Henkart P. 1995. The target cell nucleus is not required for cell-mediated granzyme- or Fas-based cytotoxicity. J Exp Med 181:1905–1909.

Natarajan V, Taher M, Roehm B, Parinandi N, Schmid H, Kiss Z, Garcia J. 1993. Activation of endothelial cell phospholipase D by hydrogen peroxide and fatty acid hydroperoxide. J Biol Chem 268:930–937.

Patton W, Pluskal W, Buecker JL, Lopez MF, Zimmermann R, Belanger LM, Hatch PD. 1990. Development of a dedicated two-dimensional gel electrophoresis system that provides optimal pattern reproducibility and polypeptide resolution. Biotechniques 8:518–527.

Patton W, Lopez MF, Barry P, Pluskal W. 1992. A mechanically strong matrix for protein electrophoresis with enhanced silver staining properties. Biotechniques 12:580–585.

Rabilloud T. 1992. A comparison between low background silver diammine and silver nitrate protein stains. Electrophoresis 13:429–439.

Ramsby M, Makowski G, Khairallah E. 1994. Differential detergent fractionation of isolated hepatocytes: biochemical, immunochemical and two dimensional gel electrophoresis characterization of cytoskeletal and noncytoskeletal compartments. Electrophoresis 15:265–277.

Sandau K, Pfeilschifter J, Brune B. 1997. The balance between nitric oxide and superoxide determines apoptotic and necrotic death of rat mesangial cells. J Immunol 158:4938–4946.

Sarafian T, Bredsen D. 1994. Is apoptosis mediated by reactive oxygen species? Free Radic Res 21:1–8.

Shepro D, Morel NML. 1993. Review: pericyte physiology. FASEB J 7:1031–1038.

Shojaee N, Patton W, Chung-Welch N, Su Q, Hechtman H, Shepro D. 1998. Expression and subcellular distribution of filamin isotypes in endothelial cells and pericytes. Electrophoresis 19:323–332.

Slater A, Stephan C, Nobel I, van den Dobbelsteen D, Orrenius S. 1995. Signalling mechanisms and oxidative stress in apoptosis. Toxicol Lett 82–83:149–153.

Song Q, Wei T, Lees-Miller S, Alnemri E, Watters D, Lavin M. 1997. Resistance of actin to cleavage during apoptosis. Proc Natl Acad Sci USA 94:157–162.

Suck D, Lahm A, Oefner C. 1988. Structure refined to 2 A of a nickle DNA octanucleotide complex with DNase I. Nature 332:464–468.

Sugiyama H, Kashihara N, Makino H, Yamasaki Y, Ota Z. 1996. Reactive oxygen species induce apoptosis in cultured human mesangial cells. J Am Soc Nephrol 7:2357–2363.

Sundaresan M, Yu Z, Ferrans V, Irani K, Finkel T. 1995. Requirement for generation of H_2O_2 for platelet-derived growth factor signal transduction. Science 270:296–299.

Suzuki Y, Forman H, Sevanian A. 1997. Oxidants as stimulators of signal transduction. Free Radical Biol Med 22:269–285.

Wood K, Youlw R. 1994. Apoptosis and free radicals. Ann N Y Acad Sci 738:400–407.